

# A DYNAMICAL SYSTEMS APPROACH TO THE DESIGN OF THE SCIENCE ORBIT AROUND EUROPA

Gerard Gomez

*Dept. Matematica Aplicada i Analisi, Universitat de Barcelona, 08 007 Barcelona, Spain*  
(gerard@maia.ub.es)

Martin Lara

*Ephemerides section, Real Observatorio de la Armada, 11 110 San Fernando, Spain*  
(mlara@roa.es)

Ryan Russell

*Jet Propulsion Laboratory, California Institute of Technology, Pasadena, CA 91109-8099, USA*  
(Ryan.Russell@jpl.nasa.gov)

## Abstract

The science orbit for a future mission to Europa requires low eccentricity, low altitude, and high inclination. However, high inclination orbits around planetary satellites are unstable due to third-body perturbations. Without control, the orbiter impacts Europa after few weeks. To minimize control, a tour over the stable-unstable, averaged manifolds of unstable frozen orbits has been suggested. We proceed with the unaveraged equations and study the manifolds of unstable orbits that are periodic in a rotating frame attached to Europa. Massive numerical computation helps in understanding the unstable dynamics close to Europa, and, thus, in selecting long lifetime high inclination orbits. A final test of a selected set of initial conditions on a high fidelity, ephemeris model, validate the results.

## 1. Introduction

The requisites of a science orbit around Europa constrain its design to high inclination, low altitude, near circular, polar orbits. Unfortunately, perturbations due to Jupiter destabilize the candidates for the science orbit about Europa. After a relatively short time, in the order of one to very few months, the orbiter will escape or impact Europa [1, 2, 3].

The underlying dynamics close to planetary satellites is well fitted to a Hill perturbed problem [4, 5]. A double averaging over the mean anomaly and the argument of the node results in an integrable system in the eccentricity and the argument of periapsis. The equilibria of the reduced system, also called frozen orbits, correspond to quasi periodic motion in the three degrees of freedom (3-DOF) problem. As both the eccentricity and the argument of periapsis remain frozen on average, orbit maintenance maneuvers reduce to a minimum. These frozen

orbits are highly desirable as nominal solutions for observation missions. However, even in the case of frozen orbits, the unstable dynamics quickly leads the orbiter to the unstable manifold of the frozen orbit. Therefore, a tour along the stable-unstable manifolds of the doubly averaged problem appears as a natural choice to enlarge the lifetime of the science orbit [6].

Among the quasi periodic orbits, periodic orbits of the 3-DOF problem indeed exist in a rotating frame attached to Europa [7, 8, 9, 10]. In theory, periodic orbits live forever. However, even the almost negligible truncation errors of the floating point arithmetic can play the role of small perturbations that reveal the natural dynamics of unstable periodic motion. After a long term propagation the orbiter eventually enters the unstable manifold of the periodic orbit, where the exponential increase in the eccentricity produces an impact of the orbiter with Europa.

As it is known from dynamical systems theory, the lifetime of the orbiter can be enlarged by taking initial conditions in the stable manifold of the periodic orbit. Note, however, that the unstable dynamics of the science mission is complex. All the branches of the manifolds must remain inside the Hill sphere, and tours using different branches of the manifolds can enjoy notably different lifetimes. To compute the longest lifetime associated to a given periodic orbit, in this work we perform a detailed study of the different branches of the stable and unstable manifolds. This atlas of trajectories can help control engineers in designing orbit maintenance routines [11].

## 2. Dynamical model

Since massive numerical computations are involved, we are compelled to choose a simplified model for our sim-

ulations. Recent research takes advantage of the small Europa to Jupiter mass ratio, and the low eccentricity and inclination of the Europa orbit, showing the accuracy of the Hill model [2, 7, 6]. Besides, as the science mission requires low altitude orbits, a second order gravity field of the central body will be considered, as already proposed by Kozai in the dawn of the Space era [4].

In a rotating frame with the origin at Europa and Jupiter to the left, the Hamiltonian of a perturbed two body problem is

$$\mathcal{H} = (1/2) (\mathbf{X} \cdot \mathbf{X}) - \boldsymbol{\omega} \cdot (\mathbf{x} \times \mathbf{X}) - \mu/r + R(\mathbf{x}), \quad (1)$$

where  $\mathbf{x} = (x, y, z)$  is the position vector,  $\mathbf{X} = (X, Y, Z)$  is the vector of conjugate momenta —velocity in the inertial frame,  $r = \|\mathbf{x}\|$ , the rotation rate of the system is  $\boldsymbol{\omega} = \|\boldsymbol{\omega}\|$ , and  $\mu$  is the gravitational parameter. System (1) is conservative and has the Jacobi constant  $C$

$$\mathcal{H}(\mathbf{X}, \mathbf{x}) = -C/2. \quad (2)$$

We consider a perturbing function  $R(\mathbf{x})$  that includes the third-body perturbation in Hill's approximation and the non-sphericity of Europa given by the gravitational harmonics expansion up to the second order. Thus, with Jupiter on the negative  $x$  axis, and taking into account the synchronous rotation of Europa with its orbital motion, the perturbing function is

$$R = (\omega^2/2) (r^2 - 3x^2) - (\mu/r) (\alpha/r)^2 (J_2/5) (7x^2 - 2y^2 - 5z^2)/r^2 \quad (3)$$

where  $\alpha$  is the equatorial radius of Europa. The second order gravitational field has been simplified by assuming the hydrostatic equilibrium condition  $C_{2,2} = (3/10) J_2$  —closely accomplished by Europa as determined from the four NASA's Galileo close encounters [12].

Note that in the standard units of the Hill problem, we can set  $\omega = \mu = 1$ . Therefore, the full Hill problem depends only on one parameter, namely the dimensional oblateness coefficient  $\tilde{J}_2 = J_2 \alpha^2$ . However, we retain more physical insight choosing units of length and time such that  $\alpha = \mu = 1$ , and maintaining  $\omega$  and  $J_2$  as parameters.

Besides the two equilibria on the  $x$ -axis, known as collinear points, the periodic solutions of the Hamiltonian Eq. (1) are of specific interest because their stability properties are easily obtained from the eigenvalues  $\lambda$  of the monodromy matrix. For periodic orbits of Hamiltonian systems the eigenvalues appear in reciprocal pairs  $(\lambda, 1/\lambda)$ , and there is one trivial eigenvalue  $\lambda = 1$  with multiplicity 2. Thus, in systems with three degrees of freedom, two stability indices  $s_i = \lambda_i + 1/\lambda_i$ ,  $i = 1, 2$ , are normally used, where  $s_i$  must be real and  $|s_i| < 2$  for linear stability.

### 3. The nominal orbit dynamics

A variety of periodic orbits in the rotating frame are known to exist around Europa, and have been previously

computed [7, 8, 9]. These periodic orbits repeat the ground trace over the surface of Europa and, for low altitudes, repeat ground-track (RGT) orbits have direct application to mapping missions.

Thus, despite the instability of high inclination orbits around planetary satellites, periodic RGT orbits have been suggested as an alternative for a long lifetime Europa science mission [13].

Ideally, periodic orbits live forever. However, numerically computed periodic orbits are periodic only within certain numerical precision  $\epsilon$ . The periodicity error together with rounding errors in the numerical integration play the role of small perturbations that shortly manifest the natural dynamics of the unstable periodic motion. This is illustrated in Fig. 1 where a polar orbit with a 40 cycle RGT delays impact to Europa to more than 400 days. However, to reach such performances the initial conditions must be determined with a precision to better than 1 mm in position and  $10^{-4}$  mm/s in velocity (periodicity error  $\epsilon \sim 10^{-11}$  in the internal units used). This is highly unrealistic from a practical point of view.

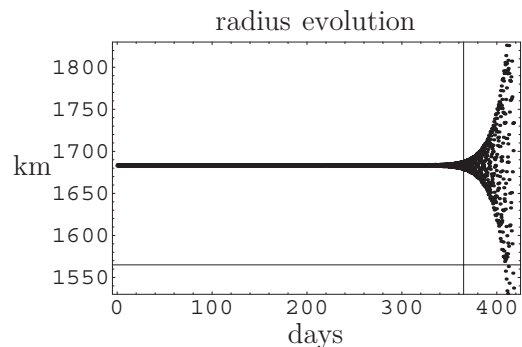


Figure 1: Long term propagation of a 40 cycle RGT, unstable, polar orbit (after [13]). The horizontal axis marks the surface of Europa.

If we assume an error on the order of 1 km in position and 1 m/s in velocity ( $\epsilon \sim 10^{-3}$ ) the lifetime then reduces to about 110 days, as shown in the top plot of Fig. 2. However, as it is known from dynamical systems theory, the lifetime of the orbiter can be enlarged by taking initial conditions on the stable manifold of the periodic orbit, as shown in the bottom plot of Fig. 2 where the lifetime extends now to more than 200 days.

### 4. Invariant manifolds computations

The computation of the invariant manifolds of a RGT science orbit presents several differences with respect to other cases, as for instance the Halo orbits around de collinear points [11] or the higher-altitude periodic orbits useful for designing ballistic captures [14]. On one side, the energy of the science orbit requires that it must be trapped around Europa, as it must occur to the whole invariant manifolds. In the units used in this paper ( $\alpha = \mu = 1$ ,  $\omega = 0.0224016$ ,  $J_2 = 4.355 \cdot 10^{-4}$ ) it corresponds to the zero velocity surface  $C = 0.300367$

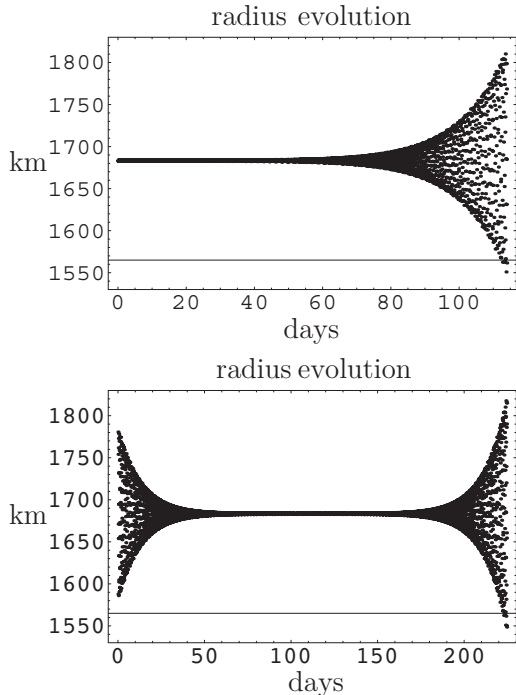


Figure 2: Top: Long term propagation of a 40 cycle RGT coarse ( $\epsilon \sim 10^{-3}$ ) periodic orbit. Bottom: improved lifetime using the stable-unstable manifold dynamics.

#### 4.1. The procedure

As has been said in the previous section, periodic orbits around the small primary are well known for the problem under consideration. In the rotating reference frame, the orbits close after completing a certain number of cycles  $P$  around Europa. For our computations, we have used orbits with values of  $P = 10, 11, \dots, 40$ .

For these periodic orbits, the values of the energy  $\mathcal{H}$  and the non-trivial stability parameter,  $s_1 = \lambda + 1/\lambda$ , are shown in Fig. 3 (the other stability parameter is always very close to 2). As it can be seen from this figure, for the values of  $P$  under consideration, all the orbits are unstable, and the instability decreases as the number of cycles increases.

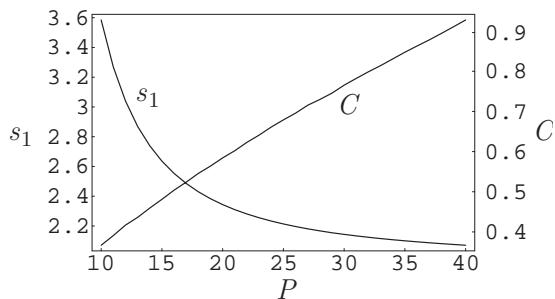


Figure 3: Jacobi constant  $C$  and stability parameter  $s_1$  of the periodic orbits

Related to the stability parameter  $s_1 > 2$ , there are the two eigenvalues of the monodromy matrix,  $\lambda > 1$

and  $1/\lambda < 1$ , which describe the hyperbolic character of the periodic orbit. The eigenvector corresponding to  $\lambda$ ,  $e^u(0)$ , gives the most expanding direction of the flow defined by the differential equations of motion, while the eigenvector associated to  $1/\lambda$ ,  $e^s(0)$  gives the most contracting direction. Once these stable and unstable directions have been computed at some initial condition of the periodic orbit ( $t = 0$ ), we can get both directions at any point of the orbit ( $t \in [0, T]$ , where  $T$  is the period of the orbit) transporting these two vectors by means of the differential matrix of the flow given by the variational equations. This is

$$e^{s,u}(t) = A(t)e^{s,u}(0), \quad t \in [0, T],$$

where  $A(t)$  is the variational matrix. These two directions, together with the direction tangent to the orbit, define the linear (local) approximations of the 2-dimensional stable and unstable manifolds of the periodic orbit. Once these local approximations have been computed, the next point is to produce the globalisation of the manifolds.

Given a displacement  $\delta$  from a selected point on the orbit  $x(t)$ , initial conditions in the linear approximation of the manifolds are given by means of

$$x^{s,u}(t) = x(t) + \delta \cdot e^{s,u}(t), \quad t \in [0, T].$$

For the computations, it is convenient to scale the stable and unstable directions  $e^{s,u}(t)$  in such a way that the norm of the vector formed by its first three components is equal to one. Then, the magnitude  $\delta$  cannot be too small in absolute value, in order to prevent rounding errors and large integration time intervals when globalising the manifolds. However, it cannot be too large because the linear approximation is useful only near the point  $x(t)$ . Values of  $\delta$  of the order of  $10^{-6}$  give good results. See [11, 14] for more detailed discussions about this point.

The two-dimensional stable and unstable manifolds (they are surfaces in the 6-dimensional space of positions and velocities) can be parametrised in the following way. As was mentioned, once a displacement  $\delta$  has been selected, given a point  $x(t)$  on the periodic orbit, we can get an initial condition on the stable/unstable manifold:  $x^{s,u}(t)$ . Following the flow backwards/forwards in time, we get all the points in the manifolds associated to  $x(t)$ . In this way  $x(t)$ , or equivalently  $t \in [0, T]$ , can be thought as one of the parameters describing the manifolds. We will refer to  $t$  as the *parameter along the orbit*. The other one is the elapsed time  $\tau$  for going, following the flow, from the initial condition  $x^{s,u}(t)$  to a certain point of the manifold  $\phi_\tau(x^{s,u}(t))$ , where  $\phi$  denotes the flow associated to the differential equations of motion. We will refer to  $\tau$  as the *parameter along the manifold*.

We remark that this parametrisation depends on the choice of  $\delta$  and the way in which the stable/unstable directions are scaled. If the scaling is done as described before, a small change in  $\delta$  produces an effect equivalent

to a small change in the parameter along the orbit. That is, with a small change in  $\delta$  we can get the same orbits of the manifold as with a small change of  $x(t)$ . Only a small shift in the parameter along the flow will be observed. This is because the stable/unstable directions are transversal to the flow.

## 4.2. Some numerical results

To illustrate the behavior of the invariant manifolds, here we will only show the results corresponding to an orbit with a 15 cycle RGT in one Europa's day. Needless to say that our conclusions are not limited to this particular orbit.

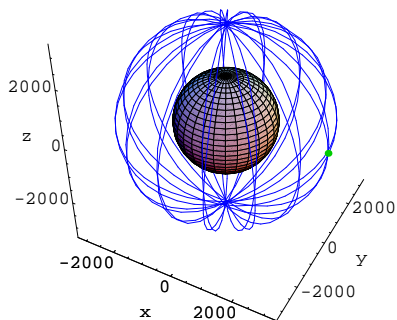


Figure 4: Periodic orbit around Europa after 15 cycles in the rotating frame. Distances are km.

We use the values  $\alpha = 1565$  km,  $\mu = 3202.7$  km<sup>3</sup>/s<sup>2</sup> and  $\omega = 2.0477 \cdot 10^{-5}$  s<sup>-1</sup> for the parameters. In internal units of length and time such that  $\alpha = \mu = 1$ , the initial conditions of the 15 cycle orbit are  $y = z = \dot{x} = 0$ ,

$$\begin{aligned} x &= 2.066698821973660, \\ \dot{y} &= -0.0699698757983462, \\ \dot{z} &= 0.6984198614672048. \end{aligned} \quad (4)$$

These initial conditions correspond to a Jacobi constant  $C \approx 0.481609$  and period  $T = 280.42701173113$ . The values of the two stability indices are  $s_1 = 2.63584$ ,  $s_2 = 2$ . In average, the orbit has semi-major axis  $a = 3242$  km, eccentricity  $e = 0.006$ , and inclination  $i = 90.5$  deg. The orbit is represented in Fig. 4, where it is clearly seen that after 15 upward crossings of the equatorial plane ( $z = 0$ ) the orbit closes.

We have done a Poincaré map representation of the stable and unstable manifolds, this is, we only display the intersections of the orbits of the manifolds with a surface of section. In this case, it has been set to be the equatorial plane  $z = 0$ , since the orbits intersect it transversally. In Fig. 5, we represent the  $x, y$  adimensional coordinates of the intersecting points with  $z = 0$  of the stable manifold. The behavior of the unstable manifold is very similar and we do not present it. In the left plot of this figure we display the first 10,000 intersections with the surface of section of 1,000 different orbits of each manifold. These orbits have been obtained taking 1,000 uniformly distributed different values of the

parameter along the orbit,  $t \in [0, 280.42 \dots]$ , associated to the manifolds. The top plot of Fig. 5 shows that the manifold intersects the surface of Europa, represented by the circle of radius one. In the bottom plot of the Figure we display only the intersections with  $z = 0$ , of the same number of orbits, before the impact with Europa. Comparing the two plots, we see that the manifold reaches the surface of Europa after a few intersections with the equatorial plane. It occurs after a relatively short time interval after the departure from the initial conditions that define their local approximation.

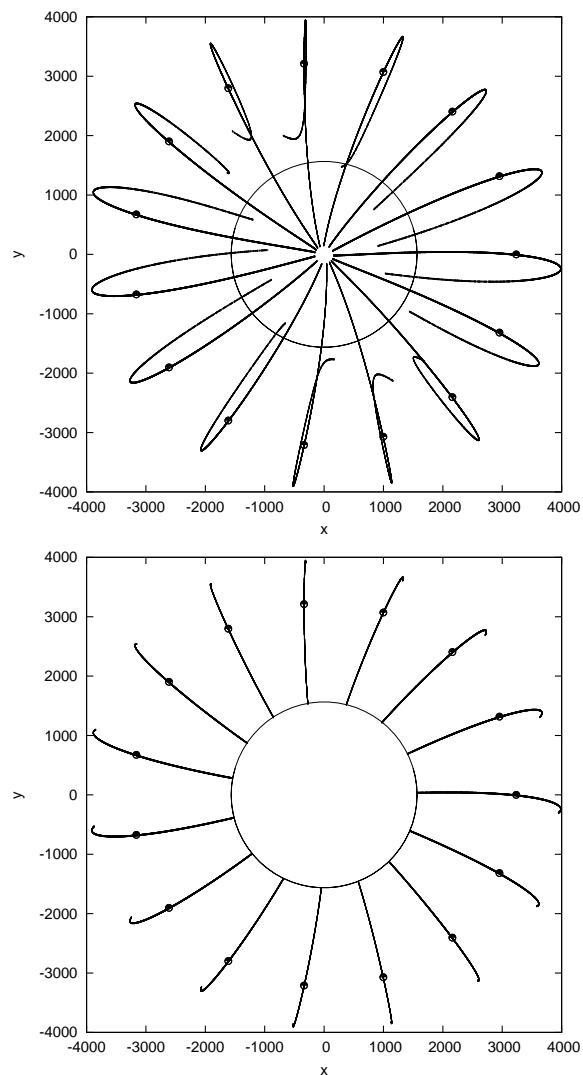


Figure 5: Top: Equatorial plane ( $z = 0$ ) crossings of the stable manifold orbits. Bottom: same plot until the impact with Europa (the circle of radius 1). The 15 large dots correspond to the initial periodic orbit.

This behavior of the manifolds explains the numerical experiments described in section 3: the orbits starting at the initial conditions of the periodic orbit do not remain on it for ever due to the numerical integration errors, the errors in the initial conditions, and hyperbolic behavior of the unstable periodic orbit. Because the manifold intersects the surface of Europa, the nu-

merically integrated orbit will also have an impact with this surface. The same phenomena appears if, instead of starting at the periodic orbit, we take initial conditions on the invariant stable manifold. Now, during a certain time interval, the orbits of the manifold will approximate asymptotically to the periodic orbit but, due to the errors in the numerical integration and the errors in the initial conditions (since we are using a linear approximation of the manifold) the orbit will finally deviate from the periodic orbit following the unstable manifold. This behavior is represented qualitatively in Fig. 6.

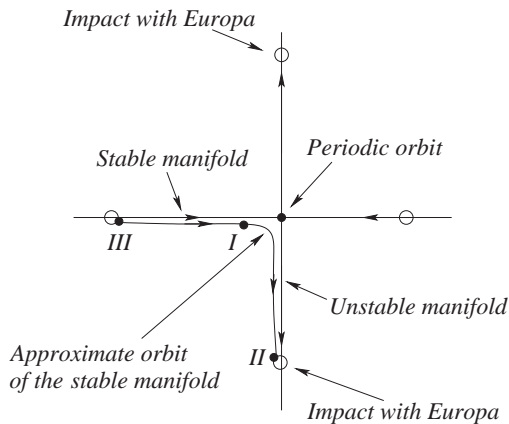


Figure 6: Qualitative behavior. The four circles on the four branches of the manifolds represent the points of the manifolds at which an impact with the surface of Europa takes place.

In Fig. 7 we give quantitative estimates of the time required for orbits of the positive branch to reach impact. The figure represents the results obtained when the initial conditions are taken on the positive branch of the stable manifold, corresponding to values of the initial conditions equal to

$$x_+^s(t) = x(t) + \delta \cdot e^s(t), \quad t \in [0, T],$$

where we fixed  $\delta = +10^{-6}$ .

The lower curve represents the time required to impact with Europa as a function of the parameter along the orbit. The initial conditions are taken at the linear approximation of the stable manifold, represented by the point labelled as *I* in Fig. 6. Clearly, there is a maximum variation of approximately 1000 adimensional time units in the time required to reach impact depending on the parameter along the orbit,  $t$ , of the manifold. Now, we can use this impact point, *II* in Fig. 6, as initial condition and integrate backwards in time, until we reach again an impact with Europa, point number *III* in Fig. 6. Taking this last point as initial condition, clearly we can enlarge by a factor of almost two the time span that we can be around the periodic orbit without impacting with Europa.

Orbits of the negative branch of the stable manifold with initial conditions  $x_-^s(t) = x(t) - \delta \cdot e^s(t)$ ,  $t \in [0, T]$ , produce almost identical results and are not presented.

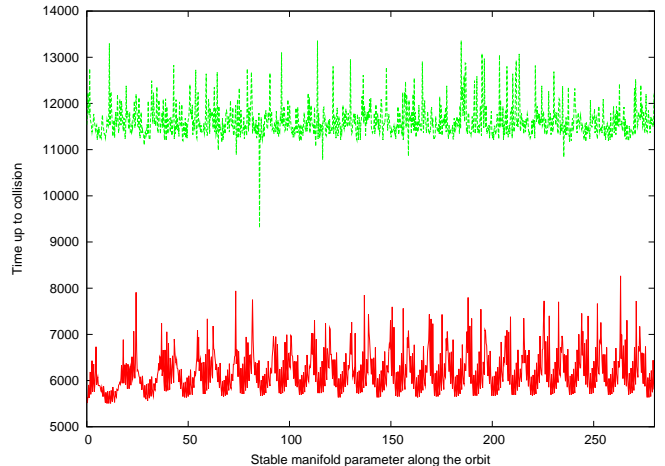


Figure 7: Orbits of the positive branch of the stable manifold of the 15 cycles periodic orbit: Time required to reach the surface of Europa starting at the stable manifold (lower curve) and between two consecutive impacts with the surface (upper curve).

## 5. The real orbit: Ephemeris runs

Tests on the validity of the solutions are made in an ephemeris model<sup>1</sup> that includes perturbations of the Sun, the other Galileans, the non-sphericity of Jupiter, the other gas giants, and the same Europa gravity field as considered in the simplified model [12]. Figure 8(a) gives the results of ephemeris propagations of the stable-unstable manifold tour based on 333 equally spaced locations along the 15-cycle reference orbit. The initial conditions are taken from the associated simplified model trajectory corresponding to points *II* and *III* from Fig. 6 for the backward and forward propagations respectively. Note, the backward and forward propagations are identical in the invariant model, but yield different trajectories in the epoch dependent ephemeris model. Each trajectory begins and ends with a Europa impact as indicated by Figure 9(b) where the radius evolution of the longest lasting orbit from Fig. 8(a), orbit A, is illustrated.

As expected, the average ephemeris lifetime is significantly less than those reported from the invariant model in Fig. 7. To further examine solution robustness and seek longer ephemeris lifetimes, in Fig. 8(c) we employ a one dimensional optimization factor that has proven useful (and explained in detail) in previous studies [8, 14]. Here, we show that the lifetime of orbit B can be significantly improved to approximate the longer lifetime enjoyed by orbit A. The narrow peak of the orbit A curve is centered at  $k = 1$ , indicating there is little room for improvement on the isolated 82 day lifetime as seen in Fig. 8(a). For comparison, initial conditions taken directly from the reference periodic orbit are optimized in a similar manner, yielding a similar lifetime profile as found for the stable-unstable tours.

<sup>1</sup>See <http://naif.jpl.nasa.gov/naif/spiceconcept.html>

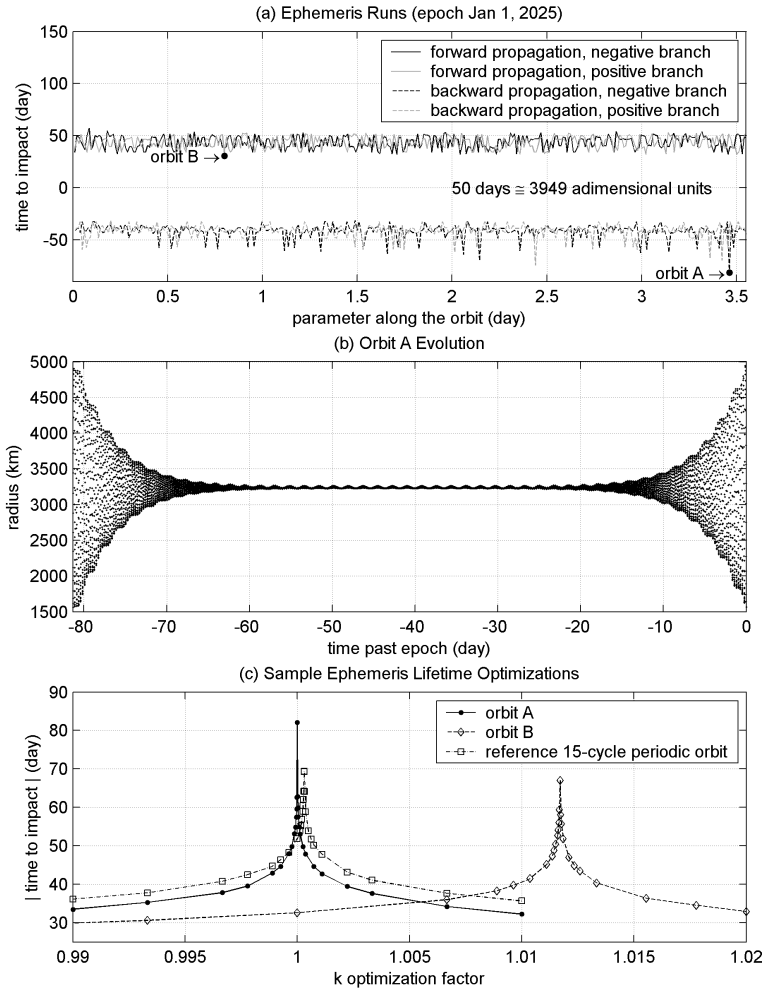


Figure 8: Selected ephemeris propagations related to the 15-cycle example periodic orbit.

## 6. Conclusions and future work

Massive numerical computations show that the real (ephemeris model) unstable dynamics around Europa is qualitatively similar to that of a simplified invariant model. This enables a methodology for computing long lifetime science orbits around planetary satellites based on stable-unstable manifold tours on selected repeat ground track orbits. Further, using the geometry of the invariant manifolds, it is possible to design a control strategy for the station-keeping of a spacecraft in the vicinity of the repeat ground track orbits. The results of this control procedure will appear elsewhere.

### Acknowledgements

Part of this work has been performed at the Jet Propulsion Laboratory, California Institute of Technology, under a contract with NASA. G.G. has been partially supported by the BFM2003-09504 grant (MCYT, Spain). M.L. acknowledges support from ESP2004-04376 and ESP2005-07107 grants (MCYT, Spain).

### References

- [1] Johannesen, J.R., D’Amario, L.A., “Europa Orbiter Mission Trajectory Design,” paper AAS 99-360, pre-

sented at 1999 AAS/AIAA Astrodynamics Specialist Conference, Girdwood, Alaska, August 1999.

- [2] Scheeres, D.J., Guman, M.D., Villac, B.F., “Stability Analysis of Planetary Satellite Orbits: Application to the Europa Orbiter,” *Journal of Guidance, Control, and Dynamics*, Vol. 24, No. 4, 2001, pp. 778–787.
- [3] Aiello, J., “Numerical Investigation of Mapping Orbits about Jupiter’s Icy Moons,” paper AAS 2005-377, presented at the 2005 Astrodynamics Specialists Conference, Lake Tahoe, California, August 2005.
- [4] Kozai, Y., “Motion of a Lunar Orbiter,” *Publications of the Astronomical Society of Japan*, Vol. 15, No. 3, 1963, pp. 301–312.
- [5] Lidov, M. L., Yarskaya, M. V., “Integrable Cases in the Problem of the Evolution of a Satellite Orbit under the Joint Effect of an Outside Body and of the Noncentrality of the Planetary Field,” *Kosmicheskie Issledovaniya*, Vol. 12, Mar.-Apr. 1974, pp. 155–170.
- [6] Paskowitz, M.E., Scheeres, D.J., “Transient Behavior of Planetary Satellites Including Higher Order Gravity Fields,” paper AAS 2005-358, presented at the 2005 Astrodynamics Specialists Conference, Lake Tahoe, California, August 2005.
- [7] Lara, M., San-Juan, J.F., “Dynamic Behavior of an Orbiter Around Europa,” *Journal of Guidance, Control and Dynamics*, Vol. 28, No. 2, 2005, pp. 291–297.
- [8] Lara, M., Russell, R., Villac, B., “On Parking Solutions Around Europa” paper AAS 2005-384, presented at the 2005 AAS/AIAA Astrodynamics Specialist Conference, Lake Tahoe, CA, August 2005.
- [9] Russell, R., “Global Search for Planar and Three-dimensional Periodic Orbits Near Europa,” paper AAS 2005-290, presented at the 2005 AAS/AIAA Astrodynamics Specialist Conference, Lake Tahoe, CA, August 2005.
- [10] Lara, M., San-Juan, J.F., Ferrer, S., “Secular Motion around TriAxial, Synchronously Orbiting, Planetary Satellites: Application to Europa,” *Chaos: An Interdisciplinary Journal of Nonlinear Science*, Vol. 15, No. 4, 2005.
- [11] Gomez, G., Llibre, J., Martinez, R., Simó, C., *Dynamics and Mission Design Near Libration Points. Vol. I Fundamentals: The Case of Collinear Libration Points*, World Scientific Monograph Series in Mathematics, Vol. 2, World Scientific, Singapore–New Jersey–London–Hong Kong, 2001.
- [12] Anderson, J.D., Schubert, G., Jacobson, R.A., Lau, E.L., Moore, W.B., Sjogren, W.L., “Europa’s differentiated internal structure: Inferences from four Galileo encounters,” *Science*, Vol. 281, 1998, pp. 2019–2022.
- [13] Lara, M., Russell, R., “On the design of a science orbit about Europa,” Paper AAS 06-168, 16<sup>th</sup> AAS/AIAA Space Flight Mechanics Conference. Tampa, Florida, USA, January 2006.
- [14] Russell, R.P., Lam, T., “Designing Capture Trajectories to Unstable Periodic Orbits around Europa,” Paper AAS 06-189, 16<sup>th</sup> AAS/AIAA Space Flight Mechanics Conference. Tampa, Florida, USA, January 2006.